

The motion of a charged particle in a fluid under a magnetic field

This article has been downloaded from IOPscience. Please scroll down to see the full text article.

1994 J. Phys.: Condens. Matter 6 9867

(<http://iopscience.iop.org/0953-8984/6/46/006>)

View [the table of contents for this issue](#), or go to the [journal homepage](#) for more

Download details:

IP Address: 171.66.16.151

The article was downloaded on 12/05/2010 at 21:05

Please note that [terms and conditions apply](#).

The motion of a charged particle in a fluid under a magnetic field

Sang Rak Kim

Physics Department, Kyonggi University, Suwon 440-760, Korea

Received 8 February 1994, in final form 22 July 1994

Abstract. The single-particle dynamics of a charged test particle in a background fluid under a magnetic field are studied using molecular-dynamics computer simulations. The off-diagonal as well as the diagonal components of the velocity autocorrelation functions (VAFs) are computed. The model interaction between the particles is a hard sphere. The diffusion constants and the Hall coefficients are also calculated at various densities. These are compared with a theory based on the projection-operator formalism. In the low density of a background fluid, the VAF can be well approximated by an exponential form. The Hall coefficients with respect to the volume fraction ν show a peak around $\nu = 0.4$, reflecting the fact that the ratio D/D_E should decrease to the value of unity from above where D_E is the Enskog diffusion constant.

1. Introduction

The velocity autocorrelation function (VAF) and its associated memory function (MF) give valuable and detailed information on single-particle dynamics [1]. The VAF is defined by $C_{\alpha\beta}(t) = \langle u_\alpha(t)u_\beta(0) \rangle$ where $u_\alpha(t)$ is the α th component of the peculiar velocity of a particle, given by $\mathbf{u}(t) = \mathbf{v}(t) - \langle \mathbf{v} \rangle$ and $\langle \dots \rangle$ denotes an appropriate ensemble average. For dense fluid, two contrasting features are involved in the VAFs. One is a long-time tail effect, which predicts that the VAF decays algebraically, leading to the enhancement of self-diffusion observed by Alder and co-workers [2] $C_{xx}(t) \propto t^{-3/2}$. This is quite different from the exponential decay expected from the Enskog theory, which assumes so-called ‘molecular chaos’, that is, that the collisions experienced by a molecule in the fluid are dynamically uncorrelated. This algebraic decay is due to the coupling between particle diffusion and shear modes in the fluid. The other feature is the back-scattering of a test particle in a cage made by the dense-background neighbours, i.e. a collective dynamical effect at short times involving many particles, leading to the decrease of self-diffusivity. In dense fluid, in principle, the diagonal components of the VAF are expected to have a long-time tail, but the amplitude is very small and so its effect can be safely neglected.

The detailed time dependences of VAFs give sufficient information for the description of macroscopic transport phenomena [3]. It is very hard to obtain them analytically due to the many-body interactions involved. Molecular-dynamics computer simulation, however, is a very powerful method to obtain VAFs [4]. Using this technique, we calculate the components of the VAF for a charged test particle in a background fluid under a magnetic field \mathbf{B} along the z direction. The time integrals of its diagonal components give the self-diffusion constants. In addition, the time integrals of its off-diagonal components characterize the dynamical correlations among molecules in dense fluids. The off-diagonal components, which are normally zero for an isotropic fluid state, become non-vanishing when we turn a magnetic field on, from which we have additional important information on the short-time dynamical behaviours of a charged particle.

2. Simulational methods

All the particles in our molecular dynamics computer simulation have a mass m and a diameter σ . They are assumed to have a hard-sphere interaction. The number of particles N is taken to be $N = 108$. To see the bulk properties we have adopted the usual periodic boundary conditions. Initially they are positioned to have a face-centred-cubic structure. The equilibration to the appropriate equilibrium fluid state is obtained after a sufficiently long time. The time averages are taken after this equilibration period.

A number of test particles (we took 10 test particles for efficiency of averaging) have an electric charge q but there is no Coulomb interaction between the charged test particles. Thus only the charged ones experience an extra Lorentzian force $F = qv \times B$ in the presence of an external field B along the z axis. For the charged particles, the next collision time with other particles should be calculated using Newton's method of root finding [5]. For all the other particles, the collision times and the velocity changes are calculated according to the usual hard-sphere molecular dynamics [6]. In the case where a magnetic field B is applied, the system does not need velocity rescaling to maintain a constant energy because there is no work actually involved. While generating the trajectories of particles, we calculated the components of the VAFs. Usually, without a magnetic field B , the off-diagonal components of $C_{\alpha\beta}(t)$ will be completely zero.

The total simulational duration is 30 000 time steps. The total number of collisions is over 70 000 at volume fraction $\eta = 0.5$. In calculating correlation functions, velocities of test particles are stored at intervals of every five steps so the number of time origins is at least 6000. Since there are 10 such test particles, we averaged over these trajectories.

All the simulational values are expressed in reduced units with mass in units of m , length in units of σ and energy in units of ε , the Lennard-Jones potential minimum parameter. The relative error of the simulated results is typically within 3%.

3. Simulational results and discussions

Consider a test particle in a system in vacuum, where the magnetic field B along the z direction is applied. Let us assume at time $t = 0$ that we have $v_x(0) = -R\omega_c \sin \phi$, $v_y(0) = R\omega_c \cos \phi$ where R is the cyclotron radius, $\omega_c = qB/m$ the cyclotron frequency and ϕ an angle measured anticlockwise from the x axis. At a later time t we have $v_x(t) = -R\omega_c \sin(\omega_c t + \phi)$, $v_y(t) = R\omega_c \cos(\omega_c t + \phi)$, $v_z(t) = v_z(0)$. Thus the VAFs can be simply written

$$\begin{aligned} C_{xx}(t) &= C_{yy}(t) = \langle v_x(t)v_x(0) \rangle = (k_B T/m) \cos(\omega_c t) \\ C_{xy}(t) &= -C_{yx}(t) = \langle v_y(t)v_x(0) \rangle = (k_B T/m) \sin(\omega_c t) \end{aligned} \quad (1)$$

and

$$\begin{aligned} C_{xz}(t) &= C_{zx}(t) = C_{yz}(t) = C_{zy}(t) = 0 \\ C_{zz}(t) &= \langle v_z^2(0) \rangle = k_B T/m \end{aligned} \quad (2)$$

where

$$(R\omega_c)^2 = 2\langle v_x^2(0) \rangle = 2k_B T/m.$$

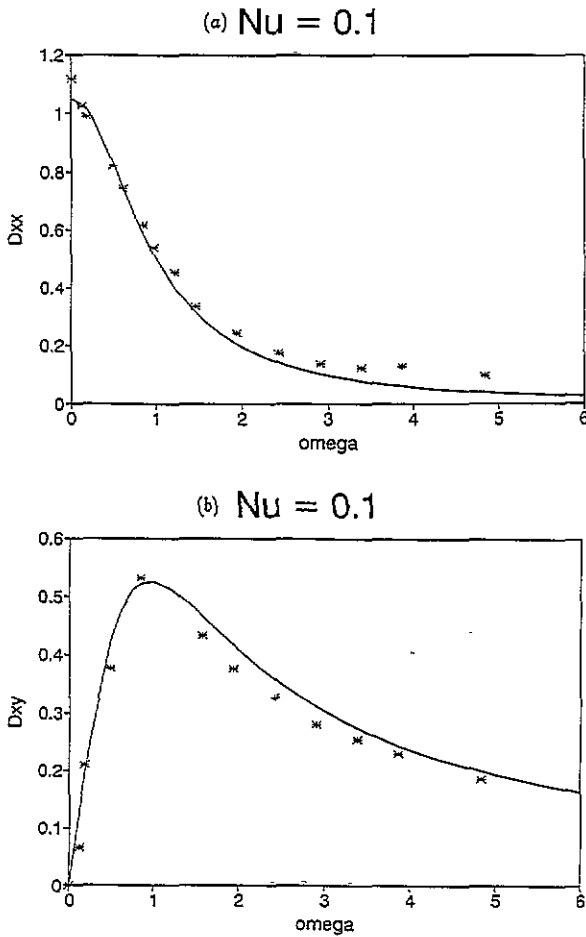


Figure 1. The diffusion constants at volume fraction $\nu = 0.1$. The solid lines represent the theoretical results. The * symbols represent the simulational results. (a) Diagonal component $D_{xx}(\omega_c)$. (b) Off-diagonal component $D_{xy}(\omega_c)$.

Thus, in vacuum, we have

$$D_{xx} = D_{yy} = D_{xy} = D_{yz} = D_{zx} = 0 \quad D_{zz} \rightarrow \infty. \quad (3)$$

This results from the fact that the charged particle is bound to move in a spiral curve about the B -field axis. However, with the background fluid present, the test charged particle experiences some collisions and thus loses its memory to give a finite value of D_{zz} and also non-zero values of D_{xx} , D_{yy} , D_{xy} and D_{yx} . In the low-density range of background fluid, if we assume the VAF to be

$$\begin{aligned} C_{xx}(t) = C_{yy}(t) &= (k_B T/m) \exp(-t/\tau_E) \cos \omega_c t \\ C_{xy}(t) = -C_{yx}(t) &= (k_B T/m) \exp(-t/\tau_E) \sin \omega_c t \end{aligned} \quad (4)$$

where τ_E is an Enskog relaxation time of the fluid, or equivalently if we assume a delta function form of the first-order MF $\delta(t - \tau_E)$, then we have

$$\begin{aligned} D_{xx}(\omega_c) = D_{yy}(\omega_c) &= (k_B T/m) \tau_E / [1 + (\tau_E \omega_c)^2] \\ D_{xy}(\omega_c) = -D_{yx}(\omega_c) &= (k_B T/m) \tau_E^2 \omega_c / [1 + (\tau_E \omega_c)^2]. \end{aligned} \quad (5)$$

Thus $D_{xx}(\omega_c)$ decreases monotonically with ω_c . Note also that $D_{xy}(\omega_c)$ has a maximum value $\frac{1}{2}(k_B T/m) \tau_E$ at $\omega_c = 1/\tau_E$. This is clearly confirmed at volume fraction $\nu = 0.1$ as shown in figure 1.

At volume fraction $\nu = 0.3$, the simulational results still confirm the theoretical proposal in (4). As shown in figure 2, however, there is more deviation from the theoretical results. With increasing cyclotron frequency ω_c , there appears an oscillatory behaviour in $C_{xx}(t)$ at $\nu = 0.3$, i.e. a backscattering effect as in the dense fluid of $\nu = 0.5$ without a field B . This reduces the overall diffusivity of the system. The simulated values of D/D_E with respect to the cyclotron frequency ω_c at $\nu = 0.3$ in fact show this remarkable behaviour in table 1.

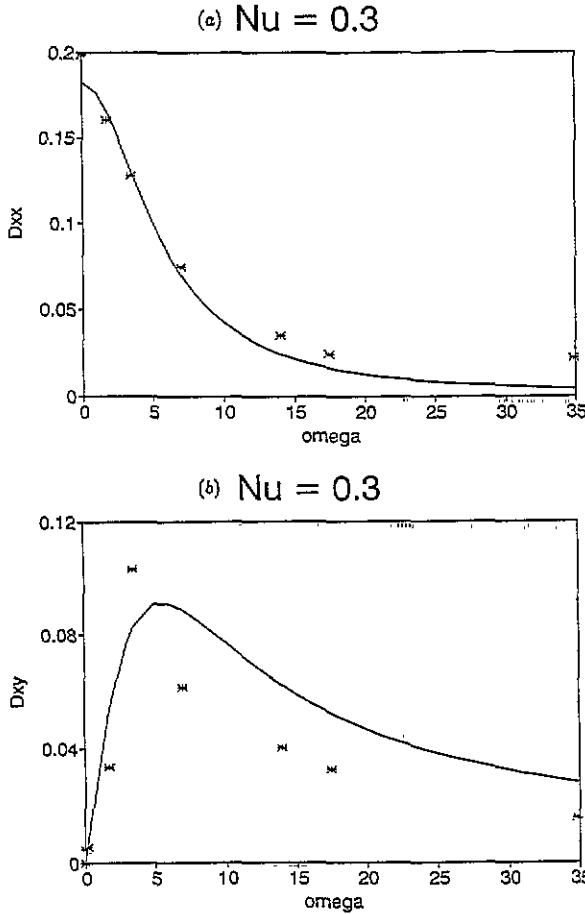


Figure 2. The same as in figure 1 except volume fraction $\nu = 0.3$.

Table 1. D/D_E at volume fraction $\nu = 0.3$.

ω_c	0	0.02	0.17	1.74	3.49	6.98	13.95	17.44
D	0.23	0.21	0.22	0.19	0.17	0.11	0.10	0.07
D/D_E	1.29	1.13	1.19	1.02	0.92	0.63	0.53	0.40

In the higher-density region, if the VAF is taken as

$$\begin{aligned}
 C_{xx}(t) &= C_{yy}(t) = (k_B T/m) \cos \omega_c t (\cos bt - (a/b) \sin bt) e^{-at} \\
 C_{xy}(t) &= -C_{yx}(t) = (k_B T/m) \sin \omega_c t (\cos bt - (a/b) \sin bt) e^{-at}
 \end{aligned}
 \tag{6}$$

where

$$\begin{aligned} a &= \frac{1}{2}(\tau_M^{-1} + \tau_E^{-1}) \\ b &= [(\tau_D^{-1} - \tau_E^{-1})\tau_M^{-1} - \frac{1}{4}(\tau_M^{-1} - \tau_E^{-1})^2]^{1/2} \end{aligned} \quad (7)$$

and $\tau_D = mD/(k_B T)$, $\tau_E = mD_E/(k_B T)$, or equivalently if the first-order MF is taken as a single exponential of the form $\exp(-t/\tau_M)$, where τ_M is the memory relaxation time of the background fluid, then the corresponding diffusion constants are calculated as

$$\begin{aligned} D_{xx}(\omega_c) &= (k_B T/m)(a/2)[(1 + |b - \omega_c|/b)/[a^2 + (b - \omega_c)^2] \\ &\quad + (1 + |b + \omega_c|/b)/[a^2 + (b + \omega_c)^2] \\ D_{xy}(\omega_c) &= (k_B T/m)\frac{1}{2}[(-|b - \omega_c|/b)/[a^2 + (b - \omega_c)^2] + (|b + \omega_c|/b)/[a^2 + (b + \omega_c)^2] \\ &\quad + 4a^2\omega_c/(a^2 + b^2)^2 + \omega_c^2(2a^2 - 2b^2 + \omega_c^2)]. \end{aligned} \quad (8)$$

At volume fraction $\nu = 0.5$, the first minimum τ_0 of $C_{xx}(t)$ occurs at $\tau_0 = 0.13$. Thus the corresponding memory relaxation time $\tau_M = 0.34$ and so the parameters $a = 9.2$, $b = 0.3$ can be obtained. It is interesting to note that at $\omega_c = b$ there are evident kinks. When $\omega_c < b$, the backscattering behaviour of short-time dynamics is dominated by the caging effect. On the other hand, when $\omega_c > b$, it is dominated by cyclotron oscillations.

When $\omega_c < b$, $D_{xx}(\omega_c)$ remains nearly constant (see figure 3(a)). In contrast, when $\omega_c > b$, $D_{xx}(\omega_c)$ increases to a maximum up to eight times that at $\omega_c = 0$. The maximum occurs around $\omega_c = 10$. Further increase of ω_c makes $D_{xx}(\omega_c)$ vanish as expected. This behaviour is quite in contrast to that of (5) for a low-density fluid.

For the case of non-diagonal diffusivity, $D_{xy}(\omega_c)$ increases almost linearly up to $\omega_c = b$. Again at $\omega_c = b$ there is a slight but somewhat different slope change. $D_{xy}(\omega_c)$ has a maximum of 0.07 at $\omega_c = 5$. Again $D_{xy}(\omega_c)$ vanishes as ω_c goes to infinity. It seems that a certain transition occurs at $\omega_c = b$ (see figure 3(b)). In contrast to the low-density cases, at volume fraction $\nu = 0.5$ there are, however, significant differences between theory and simulation as shown in figure 3(c). Since the short-time values of the VAF are obtained rather accurately in simulations, large- ω_c behaviours for diffusion constants are expected to be good.

The Hall number h is expressed as [7]

$$h = 1 - k(\tau_D^{-1} - \tau_E^{-1})^2 \quad (9)$$

where k is a memory parameter representing the three-point spatial correlation function in its explicit form. Note that from (9) h can have exactly the value of one if k is equal to zero in which case the test particle's mass is rather larger than that of a background particle, or if $D = D_E$, in which case there is no MF effect as in the Enskog approximation. Thus h is usually different from unity due to the dynamic interactions of the test particle with the background fluid particles. The Hall coefficient h is calculated at small ω_c from (9). The calculated Hall coefficient with respect to the volume fraction ν is shown in figure 4. It was expected from the theory [7] that around $\nu = 0.4$, h should have a peak, reflecting the fact that D/D_E should cross a $D/D_E = 1$ line downwards, where h should have exactly the value of one.

In the simulation, we did not change the mass of the test particle. It will be interesting to see the Brownian-ion limit, but in this limit it is more appropriate to use the Brownian dynamics method.

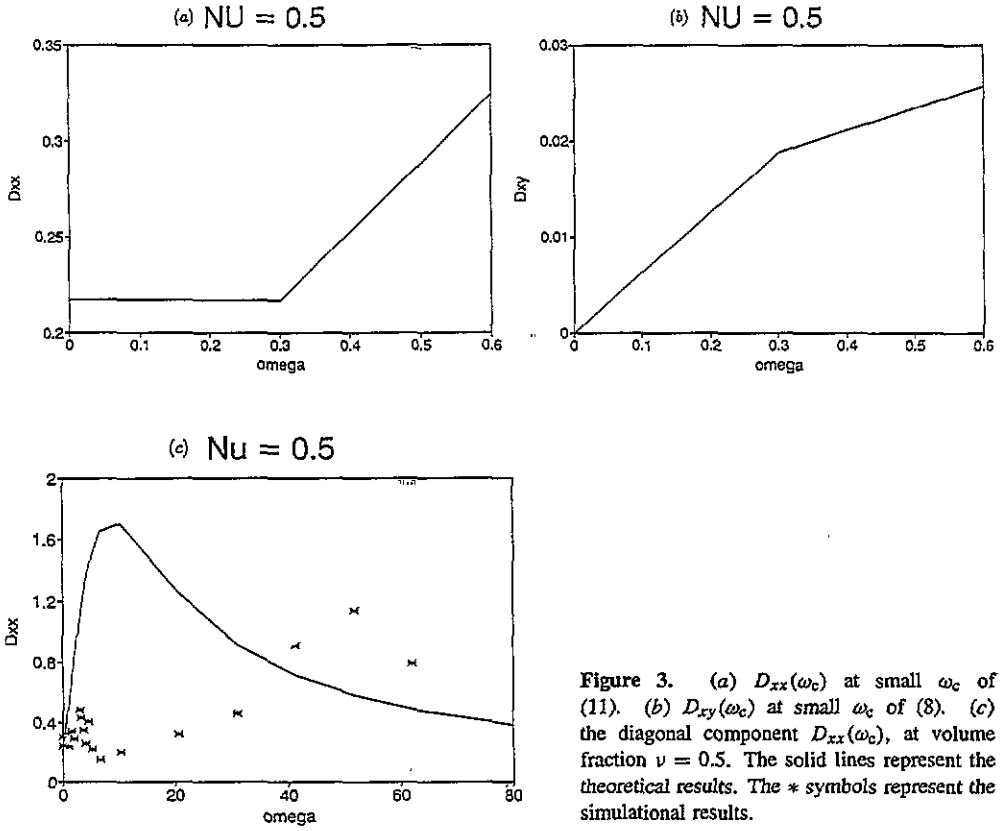


Figure 3. (a) $D_{xx}(\omega_c)$ at small ω_c of (11). (b) $D_{xy}(\omega_c)$ at small ω_c of (8). (c) the diagonal component $D_{xx}(\omega_c)$, at volume fraction $\nu = 0.5$. The solid lines represent the theoretical results. The * symbols represent the simulational results.

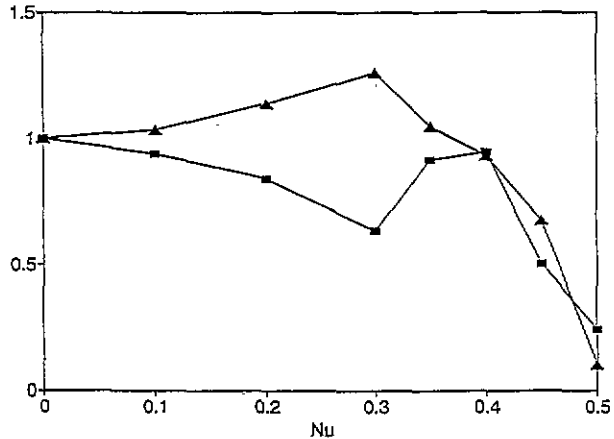


Figure 4. The Hall constant h (■) and the ratio D/D_E (▲) against volume fraction ν .

The motion in the x - y plane is quite different from the motion in the x - z plane. The motion in the x - z plane is rather similar to the motion without a field B . Fragments of circular trajectories appear in the x - y plane. This behaviour is due to the fact that between collisions the trajectories follow the motion in the vacuum. Through collisions

with background particles these circular trajectories are broken by the colliding partners. When the magnetic field is very strong, the test particles are localized and oscillating. This is quite similar to the behaviour of the glassy state.

Finally, to see these effects in molecular fluids in real experiments, we need quite a strong magnetic field of the order of magnitude at least 10^4 T, far higher than those obtainable in today's technology. However, in computer simulations we can easily access such a field by varying the parameters. This is in fact one of the great advantages of the simulational methods. Furthermore, the values of h or D_{xy} have been measured in electrolyte solutions [8] at less than 10 T. There are also some appealing macroscopic theories [9] on the Hall effect in ionic solutions.

4. Conclusion

The charged test-particle motion under a magnetic field has been studied using molecular-dynamics computer simulation. In low background fluid density the diagonal components of the VAF can be represented by a superposition of Enskog-type exponential decay and the applied cyclotron oscillation. However, in a dense system, the first-order MF can be taken to be a simple exponential type. The calculated Hall number h shows a peak around volume fraction $\nu = 0.4$ at which D/D_E approaches unity from above. For a denser fluid, h sharply decreases to zero. At volume fraction $\nu = 0.5$, the MF relaxation constant τ_M is calculated to be around 0.34. Thus our simulational results indicate that they provide a unique measure of localization or caging of the charged particle under a magnetic field in the background fluid. There is also an anisotropy of diffusion constants, and the off-diagonal component $D_{xy}(\omega_c)$ clearly has a non-zero value. However, there is, in fact a large quantitative gap between the simulational results and theoretical values in a dense liquid. Hence there should follow more elaborate theoretical developments to explain the simulational results.

Acknowledgments

I would like to thank Professor W K Sung for helpful discussions. This work has been supported in part by the KOSEF through the SRC program of SNU-CTP and through CTSP in Korea University and by the BSRIP, 1993, project No BSRI-94-2430.

References

- [1] Boon J P and Yip S 1980 *Molecular Hydrodynamics* (New York: McGraw-Hill)
- [2] Alder B J, Gass D M and Wainwright W E 1970 *J. Chem. Phys.* **53** 3813
- [3] McQuarrie D A 1976 *Statistical Mechanics* (New York: Harper & Row)
- [4] Kim S R 1990 *J. Kor. Phys. Soc.* **23** 308
- [5] Alder B and Wainwright T 1959 *J. Chem. Phys.* **31** 459
Erpenbeck J and Wood W 1977 *Statistical Physics Part B* ed B Berne (New York: Plenum) p 1
- [6] Maron M J 1982 *Numerical Analysis* (New York: MacMillan)
- [7] Sung W K and Friedman H L 1987 *J. Chem. Phys.* **87** 643; 1990 *Chin. J. Phys.* **28** 37
- [8] Gérard R, Gérard P, Meton M and Picard E-J 1983 *C. R. Acad. Sci., Paris* **297** 835
- [9] Kroh H and Felderhof B 1988 *Physica A* **153** 73; 1990 *Mol. Phys.* **70** 119